International Journal on Advanced Science Engineering Information Technology

Vol.12 (2022) No. 5
ISSN: 2088-5334

Convolutional Neural Network to Detect the Optimal Water Content of Cassava Chips During the Drying Process

Yusuf Hendrawan [a,*], Bagas Rohmatulloh [a], Fardha Irfatul Ilmi [a], Muchammad Riza Fauzy [b], Retno Damayanti [a], Dimas Firmanda Al Riza [a], Mochamad Bagus Hermanto [a], Sandra Sandra [a]

[a] *Department of Agricultural Engineering, Universitas Brawijaya, Jl. Veteran, Malang, 65145, Indonesia*
[b] *Department of Industrial Engineering, Universitas Merdeka, Jl. Terusan Raya Dieng, Malang, 65146, Indonesia*
*Corresponding author: *yusuf_h@ub.ac.id*

***Abstract*— Cassava chips are used as raw materials to manufacture modified cassava flour. To produce high-quality modified cassava flour, a drying process for cassava chips is required to produce optimal water content in the range of 15-18% wb. This study aims to detect the optimal water content of cassava chips during the drying process in a hybrid hot-air tray dryer with computer vision using a convolutional neural network. Three categories of cassava chips' water content during the drying process are wet (water content of 55-70% wb), semi-dry (20-40% wb), and optimal dry (15-18% wb). In this study, the performance of four types of the pre-trained convolutional neural network, i.e., AlexNet, GoogLeNet, ResNet-50, and SqueezeNet, were compared by using different optimizers (SGDm, Adam, and RMSProp) and different learning rate values, 0.00005 and 0.0001, resulting in 24 types of experimental design. The results showed 12 convolutional neural network models with perfect validation accuracy. AlexNet with the SGDm optimizer and learning rate of 0.00005 was determined as the best model because of its stable training iteration process that experienced no fluctuations, perfect validation accuracy, specifically 100%, as well as perfect testing accuracy was 100%, and fastest training and validation process time, notably 32 minutes. This best convolutional neural network model will later be used to develop a rapid, real-time, and accurate hybrid hot-air tray dryer with computer vision to maintain cassava chip products with optimal water content.**

***Keywords*— Cassava chips; computer vision; convolutional neural network; drying; water content.**

Manuscript received 28 Jul. 2021; revised 27 Feb. 2022; accepted 12 Apr. 2022. Date of publication 31 Oct. 2022.

I. Introduction

One of the efforts to increase food diversification is by developing the technology of modified cassava flour (MOCAF) made from cassava. MOCAF is an alternative cassava flour to replace wheat flour [1]. MOCAF is distinct from the common cassava flour, especially regarding the viscosity degree, gelling ability, rehydration power, and better solubility [2]. MOCAF is flour made from cassava that is fermented with microbes [3]. The use of MOCAF as an alternative flour to substitute wheat flour has also been proven to be a raw material for various food products such as cakes, biscuits, macaroni, noodles, bread, and analog rice [4].

The initial processing of cassava chips strongly influences MOCAF products as the main ingredient of MOCAF. High-quality cassava chips are greatly influenced by the drying process [5]. For this reason, it is necessary to build a system that can monitor and control the critical water content of cassava chips in real-time during the drying process to obtain end-products of cassava chips with optimal water content and can be used as high quality MOCAF raw materials.

The drying process of foodstuffs can affect their external appearance in terms of texture, morphology, and color. The drying process also directly affects the reduction of the water content of foodstuffs. Tegenaw [6] proved that the drying process affects changes in water content, which linearly affects the shrinkage process of the dried material. The shrinkage process directly affects the physical parameters of the dried material, such as the area, perimeter, major and minor diameter, roundness, and elongation.

Hosseinpour [7] has also proven in his research that by using a quadratic regression model, changes in the water content during the drying process have a significant effect on changes in the color of the dried material, such as lightness, redness, yellowness, browning index, hue angle, total color difference, and chroma. Jahromi [8] has observed a high correlation between color change and the water content of date-fruits chips during the drying process. The built model shows a close relationship between color change and water content of date-fruits chips with a R^2 value of 0.976 on the testing data set. Therefore, it can be concluded that the process of decreasing the water content of foodstuffs during the drying process can be identified by changes in their external appearance.

Computer vision is one of the fields of artificial intelligence that can be applied in food drying and to measure external physical parameters such as texture, size, shape, and color, which are related to measuring product quality [9]. Computer vision has been proven to be successful and effective in detecting the water content of foodstuffs as non-invasive sensing by utilizing changes in the external appearance of foodstuffs during the drying process. Li [10] have successfully developed a computer vision online measurement to measure the surface wrinkling of shiitake mushroom during hot air drying. This research proved that morphological changes had a linear effect on the water content of shiitake mushrooms during the drying process. Hosseinpour [11] has researched computer vision to monitor changes in the appearance of texture on shrimp during the drying process. In this research, computer vision was combined with Radon transform, Pseudo-Fourier-Mellin transforms, and Fourier spectrum-based fractal dimension to model the appearance of shrimp texture during the drying process.

The combination of air-drying and computer vision has been successfully applied by Raponi [12] to detect the moisture changes in the apple drying process. Sampson's use of a tray dryer with dual-view computer vision has also successfully implemented [13] to detect changes in external appearance by using the texture analysis method in the drying process of apple slices. Research on drying apple slices has also been carried out by Wang [14] and has succeeded in predicting changes in the volume of apple slices during the drying process using a combination of air-drying and computer vision. An automatic computer vision technology has also been applied for the in-line monitoring of freeze-drying processes in real-time within research by Colucci [15]. Udomkun [16] has also made a model predict color changes in papaya fruit during the drying process to control the product quality using a combination of hot-air drying and computer vision. Computer vision is one of the best alternatives to detect the water content of foodstuffs during the drying process because it has real-time, rapid, low-cost, non-destructive, and precise advantages.

An artificially intelligent system has been tested to effectively improve computer vision performance for detecting the water content of materials during the drying process. In a review study conducted by Chen [17], it can be proven that food drying to achieve optimal quality can be modeled and controlled with precision using artificial intelligence technology. Artificial intelligence can optimize and control the drying process and improve the quality of fried products, where these advantages are not found in conventional drying systems. Nadian [18] developed an intelligent integrated control on a hybrid hot-air dryer using computer vision to dry kiwi fruit. This intelligent system can significantly reduce drying load/time and balance energy consumption with product quality. Using a combination of computer vision and Bayesian extreme learning machine, Liu [19] has successfully predicted color changes in mushroom slices during the drying process.

Artificial neural network (ANN), as one of the fields of science in artificial intelligence, has been proven to be effective for predicting the water content of materials. Hendrawan and Al Riza [20] have proven the effectiveness of the combination of ANN and computer vision in modeling and predicting the water content of agricultural materials. Hendrawan [21] has also tested the performance of computer vision and ANN in modeling and predicting the water content of cassava chips during the drying process. This combination of computer vision and ANN has high accuracy. The ANN model has been tested successfully in describing the relationship between image features and water content of cassava chips during the drying process, with an R^2 value between the actual value and the predicted value of 0.9. Nadian [22] has tested the effectiveness of a continuous real-time monitoring system using a combination of ANN and computer vision on hot-air drying for drying apple slices. The results show that the combination of ANN with computer vision has satisfactorily modeled and predicted the water content of apple slices based on color input with a correlation coefficient value higher than 0.92. Fabani [23] has also built an ANN model to predict the water content of watermelon rind during the drying process. Onwude [24] has successfully monitored the shrinkage of sweet potatoes during the drying process using the ANN model and computer vision. In their research, Taheri [25] successfully predicted any changes in the water content of banana slices during the drying process in a forced convective dryer using the ANN hybrid method. Rezaei's [26] research has successfully modeled the shrinkage of potato slices due to changes in the water content of the material during the drying process in thin layer drying using ANN. The ANN 1-3-1 structure produces high prediction accuracy until the R-value attained 96.87 on the testing data set. Khazaei [27] combined computer vision with ANN to model material shrinkage due to changes in the water content of grapes during the drying process in a thin-layer dryer. The resulting model has an accuracy with a mean square error (MSE) of 0.00003 and R^2 of 0.99952 on the testing data set. Therefore, it can be concluded that the combination of computer vision supported by ANN modeling can be used to measure the water content of agricultural materials during the drying process as a non-invasive, low-cost, and precise system.

However, research has never specifically predicted foodstuff's water content during the drying process using deep learning based on a convolutional neural network (CNN). Unlike conventional machine learning methods, CNN does not require feature extraction and selection processes; thus, this method becomes more efficient, effective, and accurate [28]. In the research of Koklu [29], the superiority of CNN compared to ANN in classifying food products was proven. The classification accuracy achieved by ANN is 99.87%, while CNN achieves 100% accuracy. Jahanbakhshi [30] has proven that CNN has better performance in terms of food product classification compared to other classifier methods such as k-nearest neighbor (KNN), ANN, fuzzy, support vector machine (SVM), and decision tree. In his research, the accuracy obtained by CNN is 100%. In another study, the CNN method was also proven effective for classifying food products (cherries) with an accuracy of 99.4% [31]. Several CNN methods that have been widely used in the research of food product classification include SqueezeNet [32], AlexNet [33], GoogLeNet [34], and ResNet-50 [35]. In the research of Hendrawan [36], it was proven that pre-trained CNN using SqueezeNet, AlexNet, GoogLeNet, and ResNet-50 had a high performance for modeling and classifying the water content of agricultural materials with the highest accuracy value reaching 94.15% on the testing data set.

This study aimed to detect the optimal water content of cassava chips during the drying process in a hybrid tray dryer and computer vision using CNN-based deep learning. This study used a hot air tray dryer system equipped with a real-time computer vision system to observe changes in the water content of cassava chips during the drying process. This study used four pre-trained CNNs, namely SqueezeNet, AlexNet, GoogLeNet, and ResNet-50, tested in other studies [37]. CNN is used to classify three types of water content conditions of cassava chips during drying: wet, semi-dry, and optimal dry.

II. Materials and Methods

The material used in this research was cassava chips made from cassava sweet potato harvested from agricultural land in the area of Malang city, East Java province, Indonesia. The material preparation process included washing cassava, peeling cassava skin, then slicing cassava into thin strips with a thickness of 1 mm using a mechanical slicing machine. For the drying process, this study used a lab-scale hot-air tray dryer system (shown in Fig. 1) which was equipped with a computer vision system in real-time to observe any changes in external appearances that were affected by the shrinkage of water content during the drying process. This dryer was also equipped with a blower, electrical heating element, control unit, digital scale with an accuracy of ±0.001 g, and a drying tray.

In general, computer vision consists of digital cameras, lighting systems, computer hardware, and software. A digital camera (Logitec HD Webcam C270, Japan) was used in this study as a computer vision device placed at the height of 300 mm above the surface of the cassava chips. The digital camera was connected via a USB port connected to a computer with an Intel Core i7 processor specification. The digital camera captured digital images of cassava chips during the drying process with a resolution of 1280 × 720 and then saved them to a computer in a BMP format. The lighting factor is also crucial in computer vision. The lighting system was set equally and distributed evenly over the entire surface of the cassava chips object by using two 22W lamps (EFD25N / 22 National Corporation, Japan). The light intensity was set at 300 lux on the surface of the cassava chips. The drying process was carried out at 50-70 °C. Visual Basic 6.0-based software was used to take images automatically and save them on a computer whose time interval can be set by the user as needed.

Detailed explanation on Fig. 1 were as follows: (1) nine slices of cassava chips were placed on a tray connected to a digital scale to measure the initial weight of cassava chips; (2) cassava chips weight data was taken every 5 minutes during the drying process; (3) the digital camera took pictures of the cassava chips from the top view, along with the digital scale took the actual weight data of the cassava chips; (4) cassava chips digital image data that had been taken using a digital camera was then sent to a computer via a USB port connection; (5) CNN software in the personal computer was set to classify the water content category of cassava chips into three classes, specifically, wet (water content of 55-70% wb), semi-dry (20-40% wb), and optimal dry (water content of 15-18% wb); (6) digital image data of cassava chips with water content less than 15% were then discarded and exempted in the CNN modeling process; (7) if the results of the classification of the water content of the cassava chips had reached the optimal dry condition, then the system gave an order to the microcontroller to turn off the dryer.

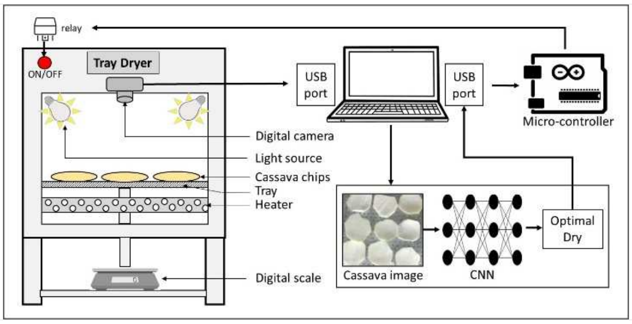

Fig. 1 Modified cassava chips tray dryer using computer vision and convolutional neural network

Fig. 2 shows the differences in external appearances on cassava chips at different water content conditions due to the drying process. On cassava chips with wet conditions, the surface was still smooth, and no shrinkage and diminution occurred; thus, the surface texture tended to look homogeneous and smooth. Visually, the color of cassava chips in wet conditions still seemed whiter. In terms of morphology, the level of roundness and perimeter still seemed round with an irregular shape. On cassava chips with semi-dry conditions, a slight shrinkage and volume shrinkage began to appear due to the reduced water content of the material. The surface texture looked inhomogeneous and coarser than cassava chips in wet conditions. In semi-dry conditions, the color started to look yellowish, which resulted in an increase in the browning index, while in terms of shape, roundness and perimeter began to change and became irregular. Cassava chips in optimal-dry conditions showed significant changes in texture, color, and shape. The texture appeared coarser and inhomogeneous, the color started to experience browning, and the shape started to become irregular.

The amount of data used in the training and validation process on CNN was 750, divided into 250 image data for the wet class, 250 for the semi-dry class, and 250 for the optimal dry class. The distribution for training and validation data was 70% training data and 30% validation data which was divided randomly [38]. In addition to the training and validation data, this study also used testing data for a total of 150 image data which were then categorized into 50 image data for the wet class, 50 image data for the semi-dry class, and 50 image data for the optimal dry class [36] [39].

(a)

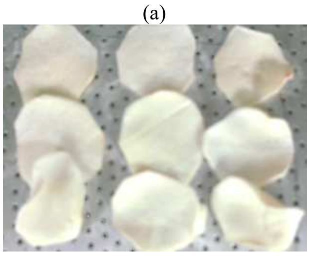

(b)

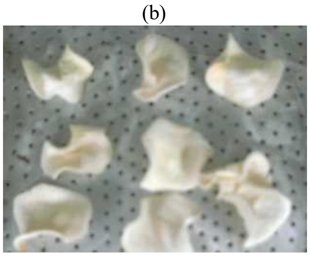

(c)

Fig. 2 The appearance of cassava chips during the drying process in various conditions of water content, such as (a) wet; (b) semi-dry; (c) optimum dryness

In general, the CNN structure used in this study is shown in Fig. 3. The CNN architecture consists of several stages: image acquisition, convolutional layer, pooling layer, and fully connected layer. Three outputs were used at the end of the CNN structure to classify the water content of cassava chips during the drying process into the wet, semi-dry, and optimal dry classes. This study used four types of pre-trained CNN, namely SqueezeNet [40], GoogLeNet [41], ResNet-50 [42], and AlexNet [33] provided in the Matlab R2020b program.

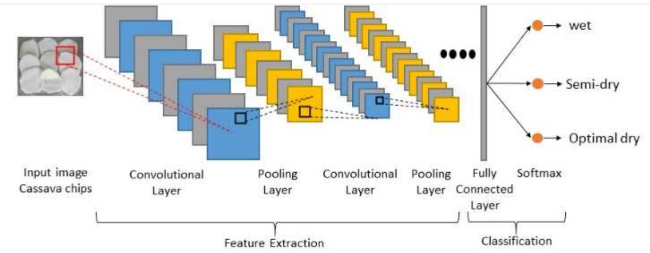

Fig. 3 CNN structure to classify the water content of cassava chips during the drying process

SqueezeNet is a pre-trained CNN consisting of 18 deep layers. The process started with resizing the image resolution to 227×227, followed by the initial convolutional layer and 8 fire modules. The initial convolutional layer in this study used was stride [2 2] and padding [0 0 0 0], while the fire modules used was stride [1 1] and padding [0 0 0 0]. The process ended with a final convolutional layer with stride [1 1] and padding [0 0 0 0]. The number of filters in each fire module always gradually increased from the beginning to the end of the network. GoogLeNet is a pre-trained CNN consisting of 22 deep layers and is a type of inception network.

The architecture of GoogLeNet uses a 1×1 convolution layer in the middle and global average pooling. The process starts by resizing the image resolution to 224×224, followed by three convolutional layers. The first convolutional layer used stride [2 2] and padding [3 3 3 3], while the second convolutional layer used stride [1 1] and padding [0 0 0 0], and the third convolutional layer used stride [1 1] and padding [1 1 1 1]. The process continued with nine inception modules and ended with a fully connected layer using three outputs. Between the inception modules and the fully connected layer, GoogLeNet implemented a drop-out layer to solve the over-fitting problem.

ResNet-50 is a pre-trained CNN consisting of 50 deep layers. The main difference between the ResNet-50 method with other pre-trained CNNs is the repeated use of residual blocks throughout the entire network. The process started by resizing the image resolution to 224×224, which was then followed by a convolutional layer using stride [2 2] and padding [3 3 3 3]. The process was continued with four residual blocks using stride [1 1] and padding [0 0 0 0]. The process ended with a fully connected layer with three outputs.

AlexNet is a pre-trained CNN consisting of 8 deep layers. The network consists of 5 convolutional layers and 3 fully connected layers. The activation function uses a rectified linear unit (ReLU). AlexNet solves the problem of over-fitting by implementing drop-out layers. The process started by resizing the image resolution to 227×227, which was then continued with convolutional layer 1 using stride [4 4] and padding [0 0 0 0]. The process continued to convolutional layer 2 using stride [1 1] and padding [0 0 0 0]. Convolutional layer 3 to convolutional layer 5 used stride [1 1] and padding [1 1 1 1]. The process continued with three stages of fully connected layers which were equipped with drop-out layers. The last fully connected layer used three outputs.

Settings on pre-trained CNN included random rotation min = 0 and max = 90 degrees; random rescaling min = 1 and max = 2; sequence padding value = 0; sequence padding direction = right; L2 Regularization = 0.00001; learn rate drop factor = 0.1; learn rate drop period = 10; and momentum = 0.9. In the training process, the maximum epoch was set at 20, the mini-batch size was 20, and the loss function used binary cross-entropy. Sensitivity analysis was carried out by varying the type of optimization method (optimizer) that referred to the research of Manninen [43]. The optimizers used include stochastic gradient descent with momentum (SGDm), adaptive moment estimation (Adam), and root means square propagation (RMSProp). Sensitivity analysis was also carried out by setting different learning rate values, namely 0.00005 and 0.0001. In the research of Thenmozhi and Reddy [44], it was shown that the learning rates of 0.0001 and 0.00005 provided the best results to be used in the CNN training process.

The training, validation, and testing processes to produce the CNN model were carried out by using a computer with specifications of Intel Core i3-4150 CPU @ 3.50GHz (4 CPUs) 10 GB of RAM. The performance of the 24 CNN models that have been built was then evaluated for the level of validation accuracy. The model with the highest validation accuracy was then tested for its performance using data testing. The data testing results were displayed using a confusion matrix [45][46].

III. Results and Discussion

Table 1 shows the classification results of cassava chips during the drying process that has been carried out by four CNN pre-trained methods, namely AlexNet, GoogLeNet, ResNet-50, and SqueezeNet. Four pre-trained CNN models were run on three types of optimizers (SGDm, Adam, and RMSProp) and two types of learning rates (0.00055 and 0.0001). Thus, 24 experimental designs were obtained. The mini-batch size configuration was 20, and the maximum epoch was 20, resulting in a maximum iteration of 520 iterations.

TABLE I
Research and Parameters Used in Pre-trained CNN

Pre-trained CNN	Optimizer	Initial learning rate	max iteration	Validation Accuracy (%)	Training Time (min)
AlexNet	SGDm	0.00005	520	100	32
	Adam	0.00005	520	99.56	33
	RMSProp	0.00005	520	100	35
	SGDm	0.0001	520	100	42
	Adam	0.0001	520	100	41
	RMSProp	0.0001	520	99.11	41
GoogLeNet	SGDm	0.00005	520	99.56	88
	Adam	0.00005	520	100	92
	RMSProp	0.00005	520	99.56	91
	SGDm	0.0001	520	100	81
	Adam	0.0001	520	99.56	66
	RMSProp	0.0001	520	100	69
Resnet-50	SGDm	0.00005	520	100	167
	Adam	0.00005	520	100	170
	RMSProp	0.00005	520	100	174
	SGDm	0.0001	520	100	173
	Adam	0.0001	520	99.56	173
	RMSProp	0.0001	520	99.11	181
SquezeeNet	SGDm	0.00005	520	100	36
	Adam	0.00005	520	99.56	39
	RMSProp	0.00005	520	99.56	49
	SGDm	0.0001	520	99.56	35
	Adam	0.0001	520	98.67	40
	RMSProp	0.0001	520	99.56	72

Based on the results of the 24 experimental designs, excellent training and validation results were obtained with a validation accuracy ranging from 99.11% to 100% with a training time range of 32 minutes to 181 minutes. The lowest validation accuracy (99.11%) was achieved when using AlexNet with the RMSProp optimizer and a learning rate of 0.0001. From the research results, it can be seen that there are 12 CNN models with perfect validation accuracy, namely 100%. The best CNN models were including AlexNet (SGDm optimizer and learning rate 0.0005), AlexNet (RMSProp optimizer and learning rate 0.0005), AlexNet (SGDm optimizer and learning rate 0.0001), AlexNet (Adam optimizer and learning rate 0.0001), GoogLeNet (Adam optimizer and learning rate 0.0001), learning rate 0.0005), GoogLeNet (SGDm optimizer and learning rate 0.0001), GoogLeNet (RMSProp optimizer and learning rate 0.0001), ResNet-50 (SGDm optimizer and learning rate 0.0005), ResNet-50 (Adam optimizer and learning rate 0.0005), ResNet -50 (RMSProp optimizer and learning rate 0.0005), ResNet-50 (SGDm optimizer and learning rate 0.0001), and SqueezeNet (SGDm optimizer and learning rate 0.0005).

Pre-trained CNN using AlexNet and ResNet-50 produced the most models with 100% accuracy, namely 4 CNN models each. However, in terms of training time, AlexNet was still superior to ResNet-50, GoogLeNet, and SqueezeNet, with an average AlexNet training time of 37 minutes, while ResNet's average training time was the longest at 173 minutes compared to AlexNet., GoogLeNet, or SqueezeNet. In general, the CNN GoogLeNet pre-trained model has the highest average validation accuracy of 99.78%, followed by AlexNet and ResNet-50 with an average validation accuracy of 99.77%, and the lowest is SqueezeNet with an average validation accuracy an average of 99.48%.

The choice of the optimizer type also affects CNN's performance. From the analysis of the 24 CNN experimental designs, the SGDm optimizer has the highest performance with an average validation accuracy of 99.93%, followed by the Adam optimizer with an average validation accuracy of 99.89%, and the last is the RMSProp optimizer with the average validation accuracy is 99.73%. The use of learning rate values also resulted in different accuracy, although not too significant. The learning rate of 0.00005 produced an average validation accuracy of 99.87%, where this accuracy value was higher than the learning rate of 0.0001, which produced an average validation accuracy of 99.85%.

The performance of the 12 best CNN models can be seen in Fig. 4. Fig. 4 shows a comparison graph between accuracy and loss. Fig. 4 displays data on training and validation values development in each iteration. Overall, the training and validation graphs shown in Fig. 4 shows a relatively similar performance pattern, e.g., there is a continuous increase in performance along with increasing iterations, where the accuracy value is increasing towards 100%, and the loss value is decreasing towards a value of 0. The performance increased very significantly at the beginning of the iteration, specifically in the range between iterations 1 to 10, which then the value increased little by little in the next iteration until it converged on the 100% accuracy value, and the loss value was 0 at the end of the iteration.

In more detail, not all training graphs listed in Fig. 4 have stable training results. In Fig. 4b, Fig. 4d, and Fig. 4g, it can be seen that the AlexNet (RMSProp optimizer and learning rate 0.0005), AlexNet (Adam optimizer and learning rate 0.0001), and GoogLeNet (RMSProp optimizer and learning rate 0.0001), have training performance that fluctuates slightly (oscillates) and is less stable. This fluctuation can be potentially caused by various factors, such as over-fitting training and validation data, insufficient datasets, noisy data, network structures that are too large, or batch size values that are too small. However, as long as this fluctuation occurred at the beginning of the iteration and this fluctuation did not occur in the other 9 best models, then this condition did not significantly affect the training performance and CNN validation for classifying the water content of cassava chips during the drying process. According to Takase [47], fluctuations in validation loss during the training process are normal in the machine learning field as long as the training pattern shows a steady increase in performance during iterations.

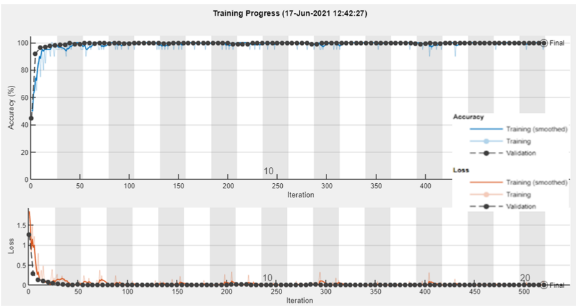

(a)

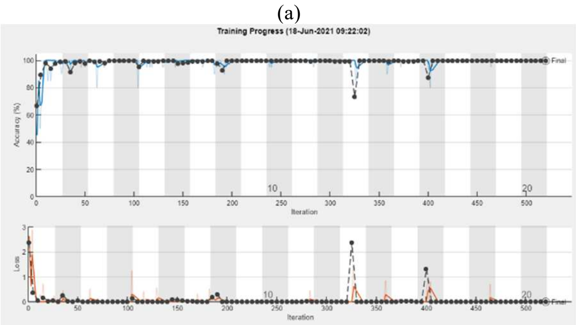

(b)

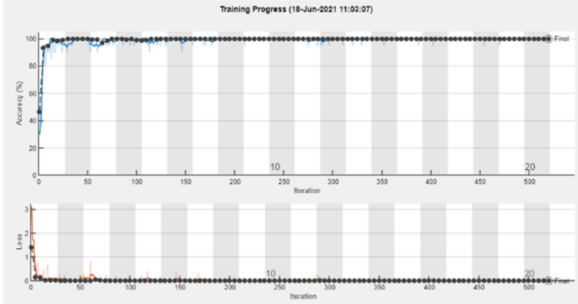

(c)

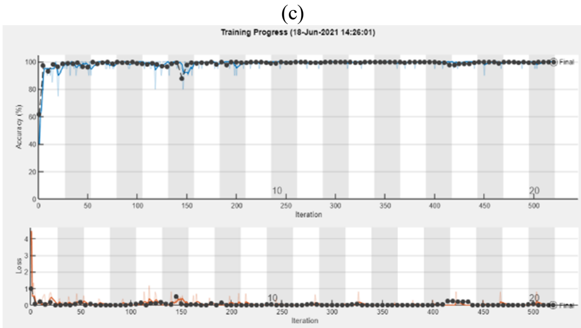

(d)

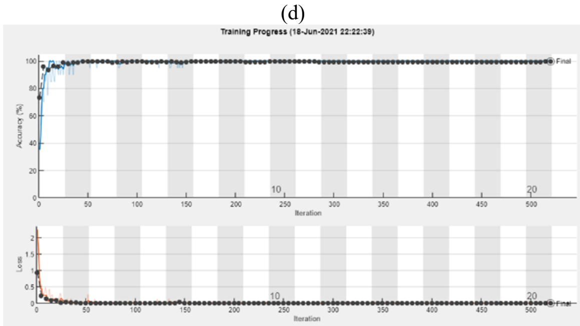

(e)

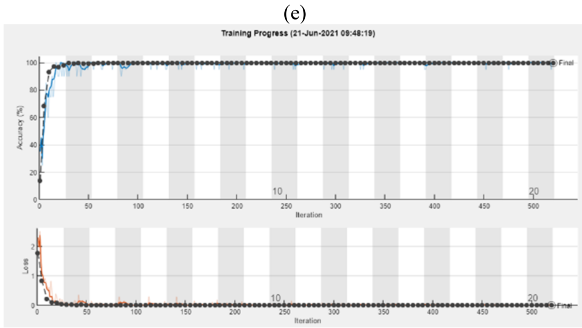

(f)

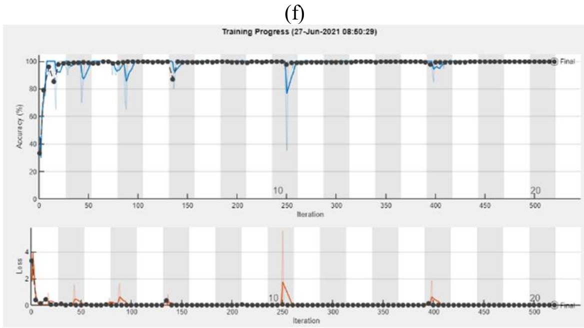

(g)

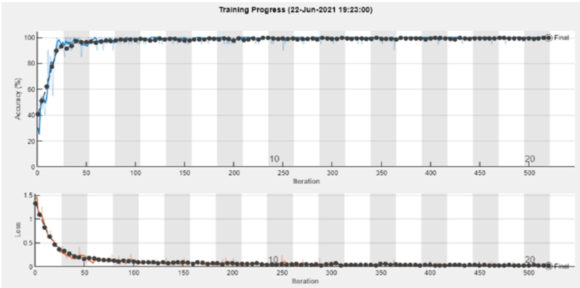

(h)

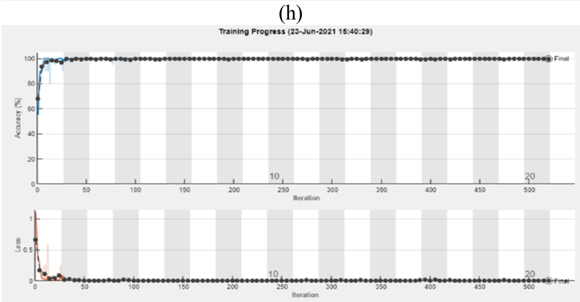

(i)

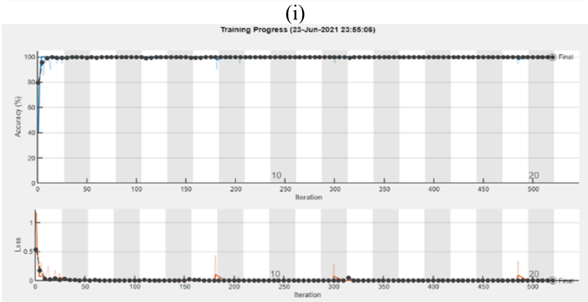

(j)

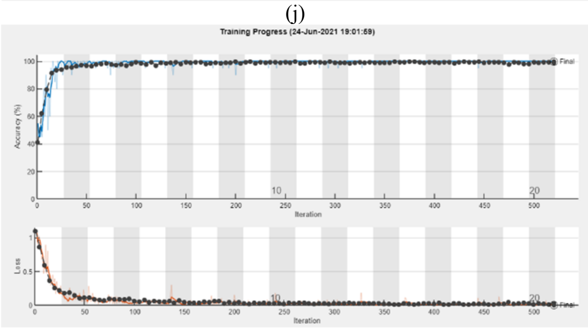

(k)

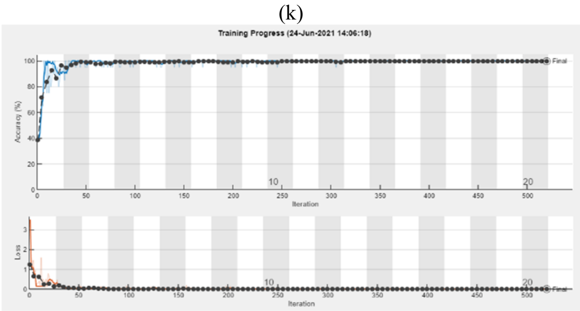

(l)

Fig. 4 Training and validation: (a) AlexNet with SGDm optimizer and learning rate 0.00005; (b) AlexNet with RMSProp optimizer and learning rate 0.00005; (c) AlexNet with SGDm optimizer and learning rate 0.0001; (d) AlexNet with Adam optimizer and learning rate 0.0001; (e) GoogLeNet with Adam optimizer and learning rate 0.00005; (f) GoogLeNet with SGDm optimizer and learning rate 0.0001; (g) GoogLeNet with RMSProp optimizer and learning rate 0.0001; (h) ResNet-50 with SGDm optimizer and learning rate 0.00005; (i) ResNet-50 with Adam optimizer and learning rate 0.00005; (j) ResNet-50 with RMSProp optimizer and learning rate 0.00005; (k) ResNet-50 with SGDm optimizer and learning rate 0.0001; (l) SqueezeNet with SGDm optimizer and learning rate 0.00005

The next stage is to test the 12 best CNN pre-trained models using testing data sets. The result is shown in Fig. 5 using a confusion matrix. The level of classification accuracy in each class of water content levels of cassava chips was described by comparing the predicted value (abscissa) and the actual value (ordinate). Testing data in this test was taken from different samples and drying times from the data used in the training and validation process. Although the test samples used were different, the results showed high accuracy in the 12 best pre-trained CNN models. Almost all CNN models showed test accuracy that reached 100%, except for one CNN model when using GoogLeNet (SGDm optimizer and learning rate 0.0001).

On the CNN model (Fig. 5f), the test accuracy for the wet class is 100%, the semi-dry is 96%, and the optimal dry is 100%. Of the 50 samples of testing data that should have been included in the semi-dry water content category, 2 samples were predicted to be included in the wet water content class, so there was an error of 4%. This could be because the external appearance of cassava chips in the wet and semi-dry classes has similar appearances. The surface texture between cassava chips at wet and semi-dry water content was rather difficult to identify because they have a smooth surface texture and are bright white in color. In terms of color appearance, cassava chips in the semi-dry water content class still did not show much browning. However, this error rate was not too significant, as long as the CNN model could still perfectly identify (100%) cassava chips in the optimal dry water content category. Thus, the CNN GoogLeNet model (SGDm optimizer and learning rate 0.0001) could still be used and be recommended to build a hybrid hot-air tray dryer with computer vision for drying cassava chips as raw material for MOCAF.

From the training, validation, and testing results, it can be concluded that the 12 best CNN models produced in this study can be used effectively to classify the water content of cassava chips during the drying process using a hybrid hot-air tray dryer with computer vision. However, if we examine further than the 12 pre-trained CNN models, even though they have the same high level of accuracy, AlexNet is highly recommended to be used as a CNN pre-trained model to classify the water content of cassava chips because of its simpler CNN structure. Therefore, the data processing time can be faster than other CNN pre-trained models such as GoogLeNet, ResNet-50, and SqueezeNet. The recommended AlexNet model in this study was AlexNet with an SGDm optimizer and a learning rate of 0.00005 for several reasons, namely a steady and stable training iteration process without any fluctuations, perfect validation accuracy of 100%, perfect testing accuracy of 100%, and the fastest training and validation process time that was 32 minutes.

By using the best CNN model from AlexNet, a rapid, real-time, and precise drying control system can be built. Thus, the quality of cassava chips as raw material for MOCAF can be maintained. This research can still be further developed to detect and classify the water content of other food products during the drying process to improve their quality and productivity.

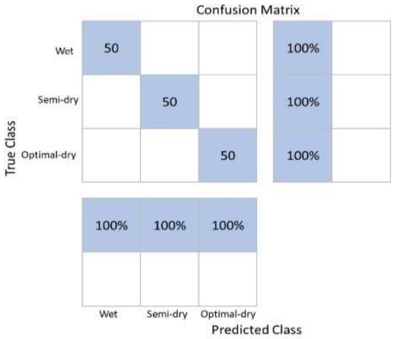
Confusion Matrix
Wet
Semi-dry
Optimal-dry
True Class
50
50
50
100%
100%
100%
100%
100%
100%
Wet
Semi-dry
Optimal-dry
Predicted Class

(a)

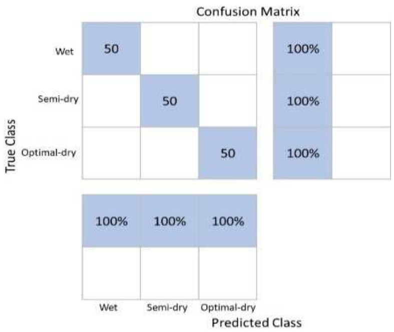
Confusion Matrix
Wet
Semi-dry
Optimal-dry
True Class
50
50
50
100%
100%
100%
100%
100%
100%
Wet
Semi-dry
Optimal-dry
Predicted Class

(b)

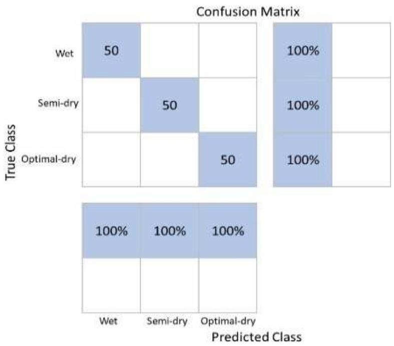
Confusion Matrix
Wet
Semi-dry
Optimal-dry
True Class
50
50
50
100%
100%
100%
100%
100%
100%
Wet
Semi-dry
Optimal-dry
Predicted Class

(c)

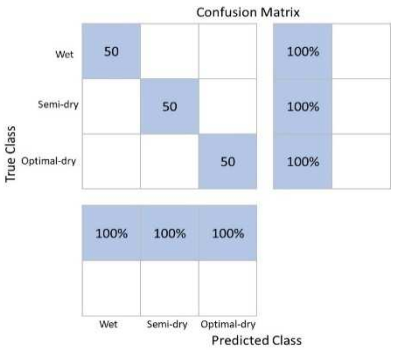
Confusion Matrix
Wet
Semi-dry
Optimal-dry
True Class
50
50
50
100%
100%
100%
100%
100%
100%
Wet
Semi-dry
Optimal-dry
Predicted Class

(d)

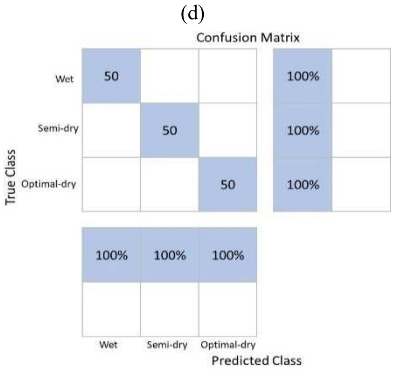
Confusion Matrix
Wet
Semi-dry
Optimal-dry
True Class
50
50
50
100%
100%
100%
100%
100%
100%
Wet
Semi-dry
Optimal-dry
Predicted Class

(e)

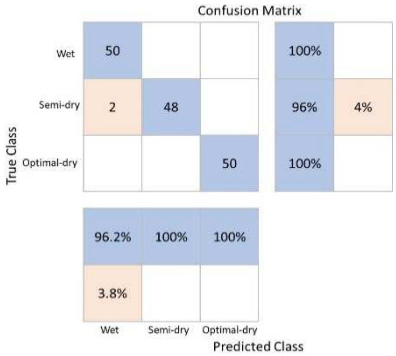
Confusion Matrix
Wet
Semi-dry
Optimal-dry
True Class
50
2
48
50
100%
96%
4%
100%
96.2%
100%
100%
3.8%
Wet
Semi-dry
Optimal-dry
Predicted Class

(f)

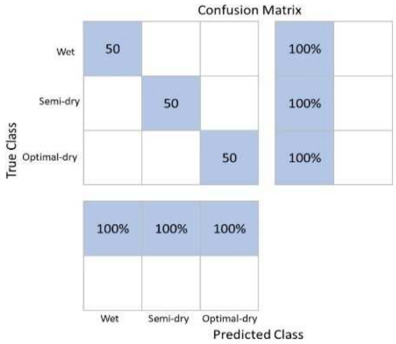
Confusion Matrix
Wet
Semi-dry
Optimal-dry
True Class
50
50
50
100%
100%
100%
100%
100%
100%
Wet
Semi-dry
Optimal-dry
Predicted Class

(g)

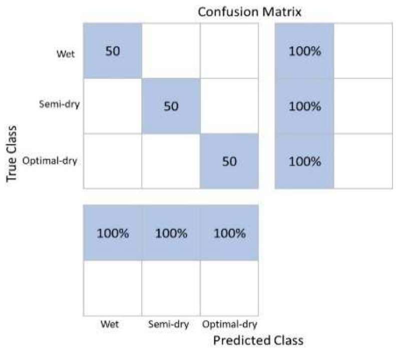
Confusion Matrix
Wet
Semi-dry
Optimal-dry
True Class
50
50
50
100%
100%
100%
100%
100%
100%
Wet
Semi-dry
Optimal-dry
Predicted Class

(h)

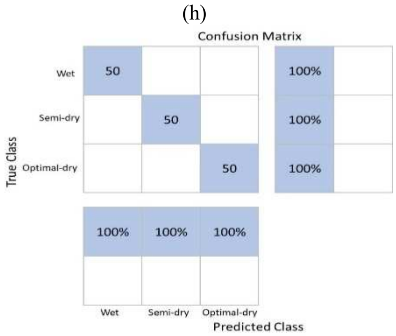
Confusion Matrix
Wet
Semi-dry
Optimal-dry
True Class
50
50
50
100%
100%
100%
100%
100%
100%
Wet
Semi-dry
Optimal-dry
Predicted Class

(i)

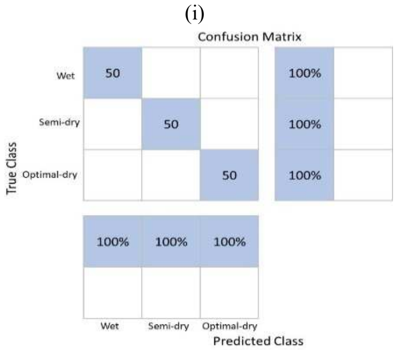
Confusion Matrix
Wet
Semi-dry
Optimal-dry
True Class
50
50
50
100%
100%
100%
100%
100%
100%
Wet
Semi-dry
Optimal-dry
Predicted Class

(j)

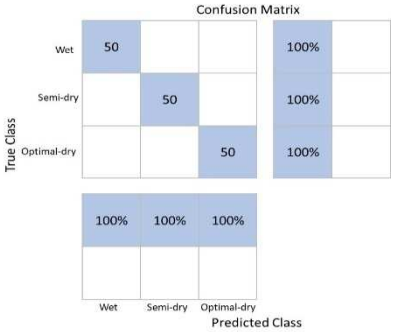

(k)

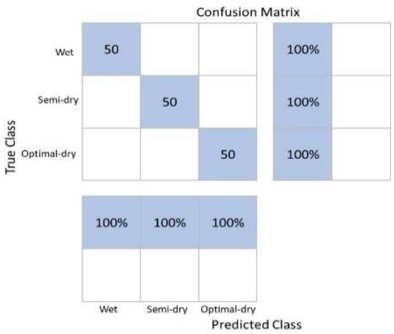

(l)

Fig. 5 Confusion matrix on testing set data: (a) AlexNet with SGDm optimizer and learning rate 0.00005; (b) AlexNet with RMSProp optimizer and learning rate 0.00005; (c) AlexNet with SGDm optimizer and learning rate 0.0001; (d) AlexNet with Adam optimizer and learning rate 0.0001; (e) GoogLeNet with Adam optimizer and learning rate 0.00005; (f) GoogLeNet with SGDm optimizer and learning rate 0.0001; (g) GoogLeNet with RMSProp optimizer and learning rate 0.0001; (h) ResNet-50 with SGDm optimizer and learning rate 0.00005; (i) ResNet-50 with Adam optimizer and learning rate 0.00005; (j) ResNet-50 with RMSProp optimizer and learning rate 0.00005; (k) ResNet-50 with SGDm optimizer and learning rate 0.0001; (l) SqueezeNet with SGDm optimizer and learning rate 0.00005

IV. Conclusion

This study aims to build a hybrid hot-air tray dryer with computer vision for drying cassava chips as raw material for MOCAF. Meanwhile, the specific objective of this study is to detect and classify the water content of cassava chips during the drying process into three classes water content: in particular wet (water content 55-70% wb), semi-dry (20-40% wb), and optimal dry (water content of 15-18% wb) using CNN. In this study, 4 pre-trained CNNs, namely AlexNet, GoogLeNet, ResNet-50, and SqueezeNet, were varied with different optimizers (SGDm, Adam, and RMSProp) different learning rate values, 0.00005 and 0.0001, resulting in 24 types of experimental designs. The results showed 12 CNN models with a perfect validation accuracy of 100%. The 12 CNN models were then tested using data testing. The results showed that 11 CNN models produced testing accuracy that reached 100%. However, from the 11 best CNN models, AlexNet with SGDm optimizer and learning rate of 0.00005 was chosen to be recommended in this study because of the steady and stable training iteration process without any fluctuations, 100% perfect validation accuracy, 100% perfect testing accuracy, and the fastest training and validation process time, which was 32 minutes. This best CNN model will later be used in developing a rapid, real-time, and accurate hybrid hot-air tray dryer with computer vision to maintain the quality of cassava chips as raw material for MOCAF.

References

[1] T. Sigüenza-Andrés, C. Gallego, and M. Gómez, "Can cassava improve the quality of gluten free breads?," *LWT*, vol. 149, p. 111923, Sep. 2021, doi: 10.1016/J.LWT.2021.111923.

[2] S. A. Oyeyinka, A. A. Adeloye, O. O. Olaomo, and E. Kayitesi, "Effect of fermentation time on physicochemical properties of starch extracted from cassava root," *Food Biosci.*, vol. 33, p. 100485, Feb. 2020, doi: 10.1016/J.FBIO.2019.100485.

[3] O. E. Dudu, Y. Ma, A. Adelekan, A. B. Oyedeji, S. A. Oyeyinka, and J. W. Ogungbemi, "Bread-making potential of heat-moisture treated cassava flour-additive complexes," *LWT*, vol. 130, Aug. 2020, doi: 10.1016/J.LWT.2020.109477.

[4] B. S. Adesina and O. T. Bolaji, "Effect of milling machines and sieve sizes on cooked cassava flour quality," *Niger. Food J.*, vol. 31, no. 1, pp. 115–119, Jan. 2013, doi: 10.1016/S0189-7241(15)30065-5.

[5] P. Pornpraipech, M. Khusakul, R. Singklin, P. Sarabhorn, and C. Areeprasert, "Effect of temperature and shape on drying performance of cassava chips," *Agric. Nat. Resour.*, vol. 51, no. 5, pp. 402–409, Oct. 2017, doi: 10.1016/J.ANRES.2017.12.004.

[6] P. D. Tegenaw, P. Verboven, and M. Vanierschot, "Numerical and experimental study of airflow resistance across an array of sliced food items during drying," *J. Food Eng.*, vol. 312, p. 110739, Jan. 2022, doi: 10.1016/J.JFOODENG.2021.110739.

[7] S. Hosseinpour, S. Rafiee, S. S. Mohtasebi, and M. Aghbashlo, "Application of computer vision technique for online monitoring of shrimp color changes during drying," *J. Food Eng.*, vol. 115, no. 1, pp. 99–114, Mar. 2013, doi: 10.1016/J.JFOODENG.2012.10.003.

[8] M. Keramat-Jahromi, S. S. Mohtasebi, H. Mousazadeh, M. Ghasemi-Varnamkhasti, and M. Rahimi-Movassagh, "Real-time moisture ratio study of drying date fruit chips based on online image attributes using kNN and random forest regression methods," *measurement*, vol. 172, p. 108899, Feb. 2021, doi: 10.1016/J.MEASUREMENT.2020.108899.

[9] Y. Su, M. Zhang, and A. S. Mujumdar, "Recent developments in smart drying technology," *Dry. Technol.*, vol. 33, no. 3, pp. 260–276, Feb. 2014, doi: 10.1080/07373937.2014.985382.

[10] X. Li, Y. Liu, Z. Gao, Y. Xie, and H. Wang, "Computer vision online measurement of shiitake mushroom (Lentinus edodes) surface wrinkling and shrinkage during hot air drying with humidity control," *J. Food Eng.*, vol. 292, p. 110253, Mar. 2021, doi: 10.1016/J.JFOODENG.2020.110253.

[11] S. Hosseinpour, S. Rafiee, M. Aghbashlo, and S. S. Mohtasebi, "A novel image processing approach for in-line monitoring of visual texture during shrimp drying," *J. Food Eng.*, vol. Complete, no. 143, pp. 154–166, 2014, doi: 10.1016/J.JFOODENG.2014.07.003.

[12] F. Raponi, R. Moscetti, S. S. Nallan Chakravartula, M. Fidaleo, and R. Massantini, "Monitoring the hot-air drying process of organically grown apples (cv. Gala) using computer vision," *Biosyst. Eng.*, Jul. 2021, doi: 10.1016/J.BIOSYSTEMSENG.2021.07.005.

[13] D. J. Sampson, Y. K. Chang, H. P. V. Rupasinghe, and Q. U. Zaman, "A dual-view computer-vision system for volume and image texture analysis in multiple apple slices drying," *J. Food Eng.*, vol. 127, pp. 49–57, Apr. 2014, doi: 10.1016/J.JFOODENG.2013.11.016.

[14] D. Wang, A. Martynenko, K. Corscadden, and Q. He, "Computer vision for bulk volume estimation of apple slices during drying," *DryingTechnology*, vol. 35, no. 5, pp. 616–624, Apr. 2017, doi: 10.1080/07373937.2016.1196700.

[15] D. Colucci, L. Morra, X. Zhang, D. Fissore, and F. Lamberti, "An automatic computer vision pipeline for the in-line monitoring of freeze-drying processes," *Comput. Ind.*, vol. 115, p. 103184, Feb. 2020, doi: 10.1016/J.COMPIND.2019.103184.

[16] P. Udomkun, M. Nagle, D. Argyropoulos, A. N. Wiredu, B. Mahayothee, and J. Müller, "Computer vision coupled with laser backscattering for non-destructive colour evaluation of papaya during drying," *J. Food Meas. Charact.*, vol. 11, no. 4, pp. 2142–2150, Dec. 2017, doi: 10.1007/S11694-017-9598-Y.

[17] J. Chen, M. Zhang, B. Xu, J. Sun, and A. S. Mujumdar, "Artificial intelligence assisted technologies for controlling the drying of fruits and vegetables using physical fields: A review," *Trends Food Sci. Technol.*, vol. 105, pp. 251–260, Nov. 2020, doi: 10.1016/J.TIFS.2020.08.015.

[18] M. H. Nadian, M. H. Abbaspour-Fard, A. Martynenko, and M. R. Golzarian, "An intelligent integrated control of hybrid hot air-infrared

dryer based on fuzzy logic and computer vision system," *Comput. Electron. Agric.*, vol. 137, pp. 138–149, May 2017, doi: 10.1016/J.COMPAG.2017.04.001.

[19] Z. L. Liu *et al.*, "Color prediction of mushroom slices during drying using Bayesian extreme learning machine," *Dry. Technol.*, vol. 38, no. 14, pp. 1869–1881, Oct. 2019, doi: 10.1080/07373937.2019.1675077.

[20] Y. Hendrawan and D. F. Al Riza, "Machine vision optimization using nature-inspired algorithms to model Sunagoke moss water status," *Int. J. Adv. Sci. Eng. Inf. Technol.*, vol. 6, no. 1, pp. 45–57, Jan. 2016, doi: 10.18517/IJASEIT.6.1.523.

[21] Y. Hendrawan, L. C. Hawa, and R. Damayanti, "Fish swarm intelligent to optimize real time monitoring of chips drying using machine vision," *IOP Conf. Ser. Earth Environ. Sci.*, vol. 131, p. 012020, Mar. 2018, doi: 10.1088/1755-1315/131/1/012020.

[22] M. H. Nadian, S. Rafiee, M. Aghbashlo, S. Hosseinpour, and S. S. Mohtasebi, "Continuous real-time monitoring and neural network modeling of apple slices color changes during hot air drying," *Food Bioprod. Process.*, vol. 94, pp. 263–274, Apr. 2015, doi: 10.1016/J.FBP.2014.03.005.

[23] M. P. Fabani, J. P. Capossio, M. C. Román, W. Zhu, R. Rodriguez, and G. Mazza, "Producing non-traditional flour from watermelon rind pomace: Artificial neural network (ANN) modeling of the drying process," *J. Environ. Manage.*, vol. 281, p. 111915, Mar. 2021, doi: 10.1016/J.JENVMAN.2020.111915.

[24] D. I. Onwude, N. Hashim, K. Abdan, R. Janius, and G. Chen, "The potential of computer vision, optical backscattering parameters and artificial neural network modelling in monitoring the shrinkage of sweet potato (Ipomoea batatas L.) during drying," *J. Sci. Food Agric.*, vol. 98, no. 4, pp. 1310–1324, Mar. 2018, doi: 10.1002/JSFA.8595.

[25] A. Taheri-Garavand, F. Karimi, M. Karimi, V. Lotfi, and G. Khoobbakht, "Hybrid response surface methodology-artificial neural network optimization of drying process of banana slices in a forced convective dryer," *Food Sci. Technol. Int.*, vol. 24, no. 4, pp. 277–291, Jun. 2018, doi: 10.1177/1082013217747712.

[26] S. Rezaei, N. Behroozi-Khazaei, and H. Darvishi, "Microwave power adjusting during potato slice drying process using machine vision," *Comput. Electron. Agric.*, vol. 160, pp. 40–50, May 2019, doi: 10.1016/J.COMPAG.2019.03.013.

[27] N. Behroozi Khazaei, T. Tavakoli, H. Ghassemian, M. H. Khoshtaghaza, and A. Banakar, "Applied machine vision and artificial neural network for modeling and controlling of the grape drying process," *Comput. Electron. Agric.*, vol. 98, pp. 205–213, Oct. 2013, doi: 10.1016/J.COMPAG.2013.08.010.

[28] H. Yu, L. T. Yang, Q. Zhang, D. Armstrong, and M. J. Deen, "Convolutional neural networks for medical image analysis: State-of-the-art, comparisons, improvement and perspectives," *Neurocomputing*, vol. 444, pp. 92–110, Jul. 2021, doi: 10.1016/J.NEUCOM.2020.04.157.

[29] M. Koklu, I. Cinar, and Y. S. Taspinar, "Classification of rice varieties with deep learning methods," *Comput. Electron. Agric.*, vol. 187, p. 106285, Aug. 2021, doi: 10.1016/J.COMPAG.2021.106285.

[30] A. Jahanbakhshi, M. Momeny, M. Mahmoudi, and Y. D. Zhang, "Classification of sour lemons based on apparent defects using stochastic pooling mechanism in deep convolutional neural networks," *Sci. Hortic. (Amsterdam).*, vol. 263, p. 109133, Mar. 2020, doi: 10.1016/J.SCIENTA.2019.109133.

[31] M. Momeny, A. Jahanbakhshi, K. Jafarnezhad, and Y. D. Zhang, "Accurate classification of cherry fruit using deep CNN based on hybrid pooling approach," *Postharvest Biol. Technol.*, vol. 166, p. 111204, Aug. 2020, doi: 10.1016/J.POSTHARVBIO.2020.111204.

[32] J. Shin, Y. K. Chang, B. Heung, T. Nguyen-Quang, G. W. Price, and A. Al-Mallahi, "A deep learning approach for RGB image-based powdery mildew disease detection on strawberry leaves," *Comput. Electron. Agric.*, vol. 183, p. 106042, Apr. 2021, doi: 10.1016/J.COMPAG.2021.106042.

[33] B. Jiang *et al.*, "Fusion of machine vision technology and AlexNet-CNNs deep learning network for the detection of postharvest apple pesticide residues," *Artif. Intell. Agric.*, vol. 1, pp. 1–8, Mar. 2019, doi: 10.1016/J.AIIA.2019.02.001.

[34] P. McAllister, H. Zheng, R. Bond, and A. Moorhead, "Combining deep residual neural network features with supervised machine learning algorithms to classify diverse food image datasets," *Comput. Biol. Med.*, vol. 95, pp. 217–233, Apr. 2018, doi: 10.1016/J.COMPBIOMED.2018.02.008.

[35] G. Ciocca, P. Napoletano, and R. Schettini, "CNN-based features for retrieval and classification of food images," *Comput. Vis. Image Underst.*, vol. 176–177, pp. 70–77, Nov. 2018, doi: 10.1016/J.CVIU.2018.09.001.

[36] Y. Hendrawan, R. Damayanti, D. F. Al Riza, and M. B. Hermanto, "Classification of water stress in cultured Sunagoke moss using deep learning," *TELKOMNIKA (Telecommunication Comput. Electron. Control.*, vol. 19, no. 5, pp. 1594–1604, Sep. 2021, doi: 10.12928/TELKOMNIKA.V19I5.20063.

[37] S. R. Nayak, D. R. Nayak, U. Sinha, V. Arora, and R. B. Pachori, "Application of deep learning techniques for detection of COVID-19 cases using chest X-ray images: A comprehensive study," *Biomed. Signal Process. Control*, vol. 64, p. 102365, Feb. 2021, doi: 10.1016/J.BSPC.2020.102365.

[38] M. Panahi, N. Sadhasivam, H. R. Pourghasemi, F. Rezaie, and S. Lee, "Spatial prediction of groundwater potential mapping based on convolutional neural network (CNN) and support vector regression (SVR)," *J. Hydrol.*, vol. 588, p. 125033, Sep. 2020, doi: 10.1016/J.JHYDROL.2020.125033.

[39] L. Bragagnolo, L. R. Rezende, R. V. da Silva, and J. M. V. Grzybowski, "Convolutional neural networks applied to semantic segmentation of landslide scars," *CATENA*, vol. 201, p. 105189, Jun. 2021, doi: 10.1016/J.CATENA.2021.105189.

[40] F. Ucar and D. Korkmaz, "COVIDiagnosis-Net: Deep Bayes-SqueezeNet based diagnosis of the coronavirus disease 2019 (COVID-19) from X-ray images," *Med. Hypotheses*, vol. 140, p. 109761, Jul. 2020, doi: 10.1016/J.MEHY.2020.109761.

[41] M. M. Raikar, S. M. Meena, C. Kuchanur, S. Girraddi, and P. Benagi, "Classification and grading of okra-ladies finger using deep learning," *Procedia Comput. Sci.*, vol. 171, pp. 2380–2389, Jan. 2020, doi: 10.1016/J.PROCS.2020.04.258.

[42] L. Mkonyi *et al.*, "Early identification of Tuta absoluta in tomato plants using deep learning," *Sci. African*, vol. 10, p. e00590, Nov. 2020, doi: 10.1016/J.SCIAF.2020.E00590.

[43] H. Manninen, C. J. Ramlal, A. Singh, S. Rocke, J. Kilter, and M. Landsberg, "Toward automatic condition assessment of high-voltage transmission infrastructure using deep learning techniques," *Int. J. Electr. Power Energy Syst.*, vol. 128, p. 106726, Jun. 2021, doi: 10.1016/J.IJEPES.2020.106726.

[44] K. Thenmozhi and U. Srinivasulu Reddy, "Crop pest classification based on deep convolutional neural network and transfer learning," *Comput. Electron. Agric.*, vol. 164, p. 104906, Sep. 2019, doi: 10.1016/J.COMPAG.2019.104906.

[45] J. Xu, Y. Zhang, and D. Miao, "Three-way confusion matrix for classification: A measure driven view," *Inf. Sci. (Ny).*, vol. 507, pp. 772–794, Jan. 2020, doi: 10.1016/J.INS.2019.06.064.

[46] Y. Hendrawan *et al.*, "Deep learning to detect and classify the purity level of luwak coffee green beans," *Pertanika J. Sci. Technol.*, vol. 30, no. 1, pp. 1–18, Dec. 2021, doi: 10.47836/PJST.30.1.01.

[47] T. Takase, "Dynamic batch size tuning based on stopping criterion for neural network training," *Neurocomputing*, vol. 429, pp. 1–11, Mar. 2021, doi: 10.1016/J.NEUCOM.2020.11.054.